



Rolling bearing fault diagnosis in strong noise background based on vibration signals

Dongjie Li^{1,2} · Mingyue Li¹ · Liu Yang¹ · Xueying Wang¹ · Fuyue Zhang¹ · Yu Liang¹

Received: 27 August 2023 / Revised: 20 September 2023 / Accepted: 13 October 2023 / Published online: 8 November 2023
© The Author(s), under exclusive licence to Springer-Verlag London Ltd., part of Springer Nature 2023

Abstract

To solve the problem of difficulty in fault feature extraction for rolling bearings under strong noise conditions, a K -value calculation method of variational mode decomposition (VMD) based on singular value kurtosis difference spectrum is proposed, which is combined with the improved maximum correlation kurtosis deconvolution (MCKD) to achieve fault diagnosis. Firstly, the singular value decomposition (SVD) algorithm is used to denoise the strong noise rolling bearing fault signals, and then, the optimal number of decomposition layers is determined according to the center frequency distance between the singular value kurtosis spectrum and the decomposed intrinsic modal function (IMF). Filtering IMFs and reconstructing faulty signals by correlation and kurtosis criteria. Optimizing the filter length L and the number of shifts M of the MCKD using the dung beetle optimizer (DBO) to enhance the signal characteristics. Finally, the envelope spectrum is used to extract the eigenfrequencies for fault diagnosis of rolling bearings and to determine the fault location. Experimentally, it is shown that the method can effectively extract the fault characteristics of rolling bearings and carry out fault diagnosis under strong noise interference.

Keywords Singular value decomposition · Variational modal decomposition · Maximum correlation kurtosis deconvolution · Dung beetle optimization algorithm · Bearing fault diagnosis

1 Introduction

As a very important part of transmission equipment, bearings are widely found in various power transmissions [1]. Bearing failure is an important factor in inducing malfunctions in mechanical transmissions, and periodic friction or impact is generated when bearings fail. Since its failure is difficult to diagnose by appearance, it is generally diagnosed by the vibration signal extracted from the acceleration sensor. However, the acquired signals are typically non-smooth, non-linear modulated signals that tend to exhibit modulation of the slow frequency on the engagement frequency [2]. Therefore, the extraction and analysis of modulated components

of these vibration signals have always been a difficult task for bearing fault diagnosis.

In recent years, signal decomposition algorithms have made good developments in gear fault feature extraction. Yang et al. performed local mean decomposition (LMD) on the collected vibration signals and extracted the characteristics of diaphragm pump check valve fault signals by Hilbert envelope spectral analysis [3]. Han et al. used the empirical mode decomposition algorithm (EMD) to decompose the vibration signal, and the time, frequency, energy characteristic parameters, and box dimensions were calculated from the time domain, frequency domain, energy domain, and fractal domain to obtain the gear fault characteristics under different load excitations [4]. Li et al. proposed a rolling bearing fault feature extraction method combining ensemble empirical mode decomposition (EEMD) and improved frequency band entropy (IFBE). A bandpass filter designed based on the frequency band entropy is used to optimize the bandwidth parameters according to the maximum envelope kurtosis principle, and a sensitive IMF reflecting the fault characteristics is selected [5]. Wang et al. combined complete ensemble empirical mode decomposition with adaptive noise

✉ Dongjie Li
dongjieli@hrbust.edu.cn

¹ Heilongjiang Key Laboratory of Complex Intelligent System and Integration, Harbin University of Science and Technology, Harbin 150080, Heilongjiang, China

² Key Laboratory of Advanced Manufacturing and Intelligent Technology Ministry of Education, Harbin University of Science and Technology, Harbin 150080, Heilongjiang, China

(CEEMDAN) with time–frequency representation demodulation analysis and proposed a strategy to reweight and reconstruct the decomposed eigenmodal functions to ensure fault feature extraction under Gaussian and non-Gaussian noise [6]. LMD, EMD, and their improved methods are adaptively decomposed, but the modal mixing problem is still difficult to solve.

The advent of variational modal decomposition has brought signal decomposition techniques to new heights [7], and it has achieved success in reducing the complexity of non-stationary signals and minimizing the effectiveness of modal aliasing. Xing et al. proposed a particle swarm algorithm based on the joint fitness function of the crag and power spectral entropy to optimize the number of decomposition layers and the penalty factor of the variational modal decomposition, select the mode with the highest energy for signal reconstruction, and apply the Hilbert transform to obtain the time difference of the echo signal [8]. Ji et al. proposed the energy difference and correlation coefficient as the criterion for the number of modal decompositions in VMD and improved the interval sampling energy operator to quickly extract the instantaneous amplitude and frequency of harmonics, realizing the fast and accurate measurements of non-stationary harmonic time–frequency parameters [9]. In feature extraction, the envelope entropy of the vibration signal is an important indicator for determining bearing faults. Tan et al. proposed a hybrid framework based on Multi-Envelope Teaching Optimization (METLBO) by combining parametric optimization variational modal decomposition with an improved support vector machine (ISVM) [10]. An improved parametric adaptive variational modal decomposition is proposed by Miao et al. A new integrated kurtosis index is constructed by combining kurtosis and envelope spectral kurtosis. The mean value of the ensemble kurtosis of all modes is selected as the objective function, and an iterative algorithm is used to extract all potential fault information [11]. However, there is room for improvement in the determination of the optimal number of decomposition layers K for modal decomposition.

To address the problem of fault feature enhancement, in 2012, McDonald et al. proposed maximum correlation cliff deconvolution based on minimum entropy inverse fold product, which can significantly enhance the shock component of the fault signal [12]. In recent years, MCKD has been widely used for fault diagnosis of gear, bearing, and other rotating machinery components [13, 14]. Chen et al. used the MCKD technique for signal noise reduction to enhance the energy amplitude of components related to planetary bearing faults and improved the feature optimization map to improve the envelope spectrum to effectively extract bearing fault vibration components [15]. He et al. proposed the maximum correlation kurtosis inverse fold product as an effective means to identify periodic pulses of fault signals and filter

out bearing fault information using the envelope spectrum generated by the correlation kurtosis index [16]. Meanwhile, for the parameter selection problem in MCKD, some intelligent optimization algorithms, including gray wolf optimizer (GWO) [17], sparrow search algorithm (SSA) [18], and dung beetle optimizer (DBO) [19], play an important role. Jun et al. used an artificial fish swarm algorithm to optimize the filter length L and shift number M in MCKD to achieve a multi-fault diagnosis of bearings [20]. Song et al. combined the sample entropy and crag index to construct the minimum entropy crag ratio and used genetic algorithms to search for the minimum value of the minimum entropy crag ratio to determine the optimal parameter combinations of the number of shifts, filter lengths, and periods, and to realize the effective extraction of weak fault features [21].

Therefore, to solve the problem that the determination of parameter K in VMD is too dependent on the a priori knowledge, an optimal decomposition layer calculation method based on SVD is proposed, and for the problem that it is difficult to identify the weak fault features in the background of strong noise, DBO is used to optimize the L , M parameter of MCKD to enhance the fault features of vibration signals. Determine the optimal number of decomposition layers of VMD to decompose the vibration signal using the singular value kurtosis difference spectrum. The IMF reconstructed signals are screened according to the correlation coefficient criterion and the kurtosis index, and the weak pulse features are enhanced using the MCKD optimized by the DBO algorithm. Fault diagnosis is carried out by analyzing the fault frequency of the envelope spectrum of the bearing signal, and simulation and experimental analysis verify the effectiveness of the method in bearing fault diagnosis.

2 Basic theory

2.1 Optimal K -value algorithm based on SVD

VMD is based on the adaptive property of signal decomposition, which depends on the frequency information of the signal. The real-valued signal is decomposed into K eigenmode functions by VMD, and the choice of the value of K has a great influence on the decomposition result. When the value of K is too small, it results in incomplete decomposition. And when the value of K is too large, it results in over-decomposition. Therefore, the distance between the center frequencies of adjacent IMF components is calculated using the following equation:

$$\min \left(\left| \frac{\omega_{i+1} - \omega_i}{(\omega_{i+1} - \omega_i)/2} \right| \right) \leq \gamma \quad (1)$$

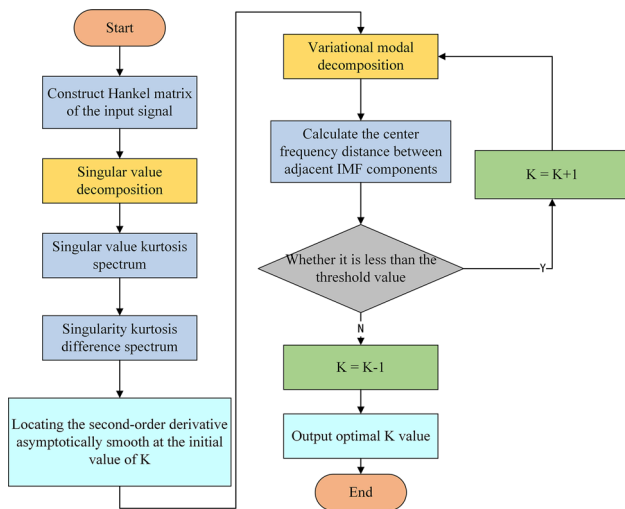


Fig. 1 Flow chart for calculating the optimal number of decomposition layers

where ω_i, ω_{i+1} are two similar center frequencies, γ is a constant and is set to 0.1.

Singular value decomposition has the ability of noise filtering, interference insensitivity, and high-resolution spectral decomposition. Singular values in a signal often carry important information, and it is one of the important features of the signal. The difference between neighboring singular values in a singular value matrix can be defined by the singular value difference spectrum, and the formula for neighboring singular value difference is as follows:

$$b_i = \sigma_i - \sigma_{i+1}; (i = 1, 2, \dots (n - 1)) \tag{2}$$

The sequence composed of b_i is called the singular value kurtosis difference spectrum. When the neighboring singular values are different, a peak appears in the singular value difference spectrum, i.e., a mutation occurs. The location of the mutation is used to find out where the original signal is converted from a useful signal to a noise signal. Kurtosis is very sensitive to the shock characteristics of the signal, when the rolling bearing occurs local failure, the vibration signal will have shock characteristics, so kurtosis can be used as the basis for selecting the effective singularity.

In summary, an improved SVD-based method for calculating the optimal K value is proposed in Fig. 1.

2.2 Correlation and kurtosis metrics

After the original signal is decomposed into K IMFs, the IMFs are often filtered using the correlation principle. The strength of the correlation between the IMF and the original signal is determined by calculating the correlation coefficient between the IMF and the original signal. Assuming that x and y are two time-domain signals, the correlation coefficient r_{xy}

is calculated as follows:

$$r_{xy} = \frac{\sum_{i=1}^N (x_i - \bar{x})(y_i - \bar{y})}{\sqrt{\sum_{i=1}^N (x_i - \bar{x})^2 \sum_{i=1}^N (y_i - \bar{y})^2}} \tag{3}$$

where N is the length of the signal; \bar{x} and \bar{y} are the mean values of signal x and y .

Since the correlation coefficient is greatly affected by noise, the kurtosis index is added to the screening. According to experience, the signal kurtosis is close to 3 when the normal bearing is running, and when the bearing fails, the signal kurtosis will be larger than 3. In this paper, we calculate the correlation coefficient and kurtosis value between each IMF and the original signal and filter out the IMF components that satisfy the correlation coefficient larger than the threshold value and the kurtosis larger than 3 at the same time for the reconstruction of the signal.

2.3 Optimization of DBO-based signal enhancement algorithm

The MCKD algorithm can effectively extract the periodic shock pulse components, and its solution process is a process of solving the optimal solution of the FIR filter. To verify that the signal recovered by this filter satisfies the periodic shock characteristics, it is necessary to utilize the associated cliff metric. The signal is filtered and the filter solved is the one that satisfies the requirements when the correlation cliff $CK_M(T)$ is maximized. The algorithm has 3 important parameters T, L , and M .

In this paper, we use the DBO algorithm to optimize the L and M parameters of MCKD, using the sample entropy as the objective function. Set the population size $N = 30$, the number of iterations $n = 50$, the range of values of L is [100, 500], and the range of values of M is [1, 7] in the DBO algorithm. The DBO optimization of the MCKD algorithm is performed to find the best combination of (L, M) by taking the minimum value of the sample entropy of the effective component as the objective function. Where the sample entropy is calculated as

$$SampEn(m, r) = \ln B^m(r) - \ln A^m(r) \tag{4}$$

where $B^m(r)$ is the average value of the ratio of the approximate number of signal sequences to the total number, and $A^m(r)$ is the average value of the ratio of the approximate number of signal sequences to the total number after adding 1 to the dimension.

2.4 Fault diagnosis process

This paper proposes a bearing fault diagnosis method based on improved variational modal decomposition and envelope

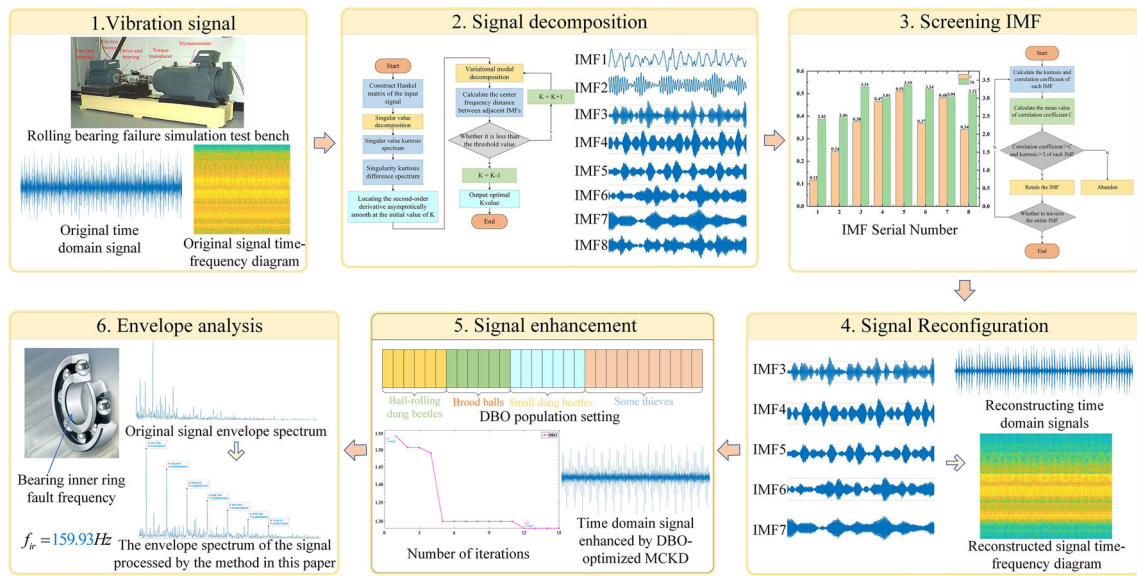


Fig. 2 Bearing fault diagnosis flow chart

spectral analysis, and the structural flowchart of the fault diagnosis method is shown in Fig. 2. The main algorithmic process consists of the following steps: Firstly, the vibration signals are acquired; the original signals are denoised based on the singular value kurtosis difference spectrum, and the optimal number of signal decomposition layers K is determined; the vibration signals are decomposed by the VMD and screened; the IMFs that meet the correlation and kurtosis indexes are used for signal reconstruction; the reconstructed signals are augmented with the MCKDs optimized by the dung beetle optimization algorithm; the augmented signals are demodulated by the envelopes and analyzed for the frequency of the faults.

3 Simulation signal analysis

To verify the effectiveness of the method, simulated signals are created and analyzed in this paper. To simulate the strong noise operating environment of the bearing, a Gaussian noise signal with a signal-to-noise ratio of -14 dB is added to the pulse signal to form the analog signal. The final analog signal is shown in Eq. (5):

$$\begin{cases} x(t) = s(t) + n(t) = \sum_i A_i h(t - iT) + n(t) \\ h(t) = \exp(-Ct) \cos(2\pi f_n t) \\ A_i = 1 + A_0 \cos(2\pi f_r t) \end{cases} \quad (5)$$

where $s(t)$ is the periodic shock part; the amplitude A_0 is 0.3; the rotation frequency f_r is 30 Hz; the attenuation coefficient C is 700; the resonance frequency f_n is 4 kHz; the inner ring fault characteristic frequency $f_i = 1/T = 120$ Hz; $n(t)$ is the

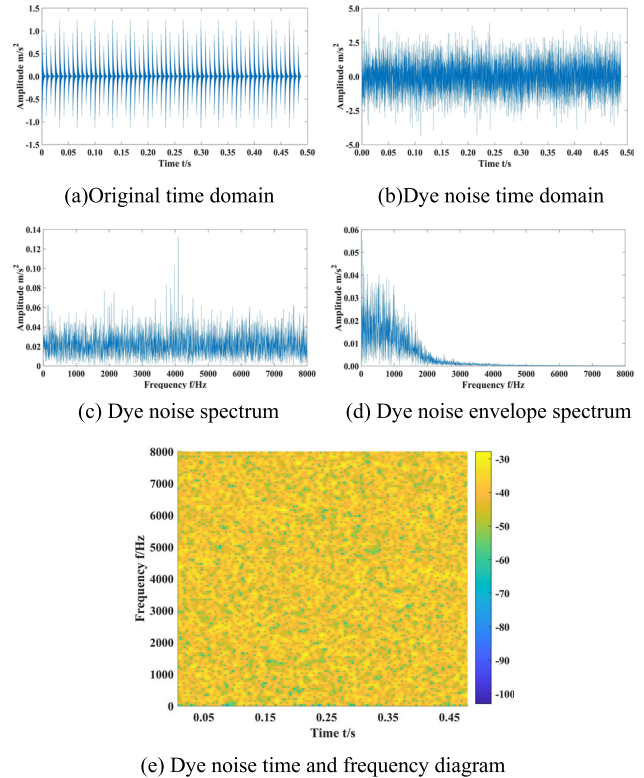


Fig. 3 Analog signal waveform diagram

Gaussian white noise component; the sampling frequency f_s is 16 kHz; and the number of analysis points is 4096.

Figure 3a shows the time domain diagram of the simulated signal, and it can be seen from the figure that the simulated signal shows an obvious periodic variation.

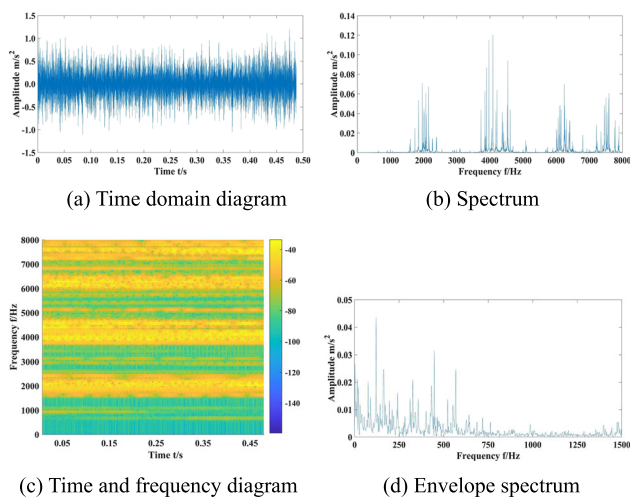


Fig. 4 Reconstructed signal waveform diagram

The time domain plot and spectrum of the signal after adding -14 dB of random Gaussian white noise are shown in (b) and (c) in Fig. 3. The signal characteristics are almost completely drowned out after noise contamination, and the pulse frequencies are hidden by the noise, the resonant frequencies are also vaguely visible. Figure 3d shows the envelope spectrum of the simulated signal after noise staining. The fault frequencies and their multiples in the figure are masked by noise and are indistinguishable.

(e) is a time–frequency plot of the dyed-noise signal, with a large number of noise points in the plot.

The optimal number of decomposition layers $K = 10$ for the analog signal is determined using the method proposed in Sect. 2.1. IMF3, IMF6, IMF7, IMF9, and IMF10 that satisfy a crag greater than 3 and a correlation coefficient greater than the mean value of 0.33 were screened for signal reconstruction.

The time domain plot spectrum and the time–frequency analysis spectrum of the reconstructed signal are shown in Fig. 4a and b. Compared with the original analog signal, the burr and noise bands in the reconstructed signal are much reduced, and the noise reduction effect is obvious. To visualize the noise reduction effect, a time–frequency analysis of the signal is shown in Fig. 4c. Comparing with Fig. 3e, it is found that the noise in high and low frequencies has been eliminated substantially. That is, most of the high and low-frequency noise is eliminated, but a small amount of noise still exists. Figure 4d shows the envelope spectrum of the reconstructed signal. The fault frequencies and their multiples can already be seen in the figure, but they cannot be clearly extracted and there are many interfering spectral lines.

The time-domain and envelope spectra of the signals processed by the method of this paper are shown in Fig. 5a and b. The frequency at the maximum peak in the plot is chosen as

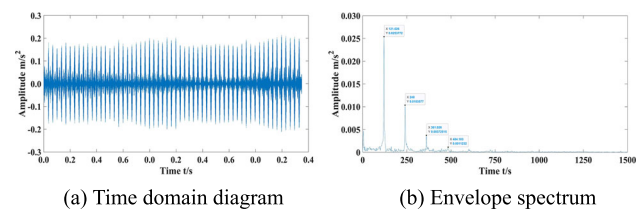


Fig. 5 Time domain and envelope spectra of the signal processed by this method

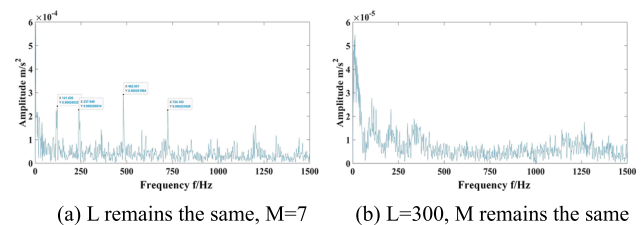


Fig. 6 Envelope spectrum after changing MCKD parameters

the characteristic frequency f_i , so $f_i = 120$. The DBO algorithm is used to optimize the parameters L and M of MCKD. The population number of the DBO algorithm is set to 100, the maximum number of iterations is 10, and the objective function of parameter optimization is the minimum value of sample entropy. At the 6th iteration, the optimal parameters are found to be [243, 1]. Therefore, the parameters $L = 243$, $M = 1$, and $T = 75$ are set for the MCKD algorithm. The characteristic spectral lines in the figure are very prominent, and the characteristic frequency f_i of the fault and its multiples can be easily identified, thus confirming the effectiveness of the proposed diagnosis method.

To verify the rationality of using the DBO algorithm to optimize the parameters L and M of MCKD, we now change the parameters of M and keep L constant to observe the results. The signal envelope spectrum analyzed by the MCKD algorithm with random order $M = 7$ and $L = 243$ is shown in Fig. 6a. As can be seen in Fig. 6a, compared to the optimal combination of L and M , when only L is guaranteed to be at the optimal value, the amplitude of the envelope spectrum of the signal processed by the method in this paper is small and reduced to about one percent of the original one. Then keeping the value of M constant and changing the value of L , that is, taking $L = 300$ and $M = 1$ randomly, the signal envelope spectrum analyzed by the MCKD algorithm is shown in Fig. 6b. In Fig. 6b, there are numerous interference spectral lines, which make it difficult to identify the fault frequency and its multiplication information. It shows the reasonableness of the results of parameters L and M of MCKD optimized by DBO in this paper.

Table 1 Bearing failure information

Fault location	Fault frequency calculation formula	Theoretical value of fault frequency
Bearing inner ring	$f_{ir} = \frac{N}{2} (1 + \frac{d}{D} \cos \theta) f_r$	$f_{ir} = 162.19 \text{ Hz}$
Bearing outer ring	$f_{or} = \frac{N}{2} (1 - \frac{d}{D} \cos \theta) f_r$	$f_{or} = 107.30 \text{ Hz}$

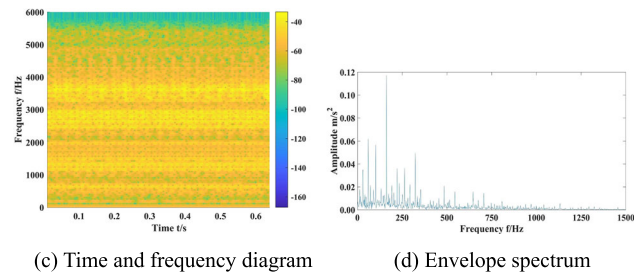
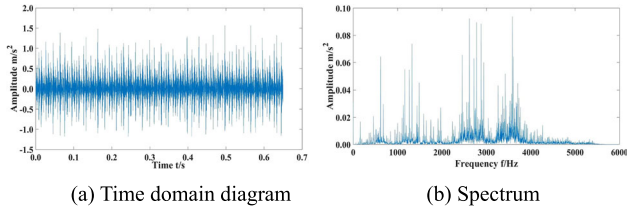


Fig. 7 Bearing failure signal waveform diagram

4 Measured signal analysis

4.1 Data source

To verify the effectiveness of the method in this paper, the test data from the publicly available rolling bearing failure simulation platform at Case Western Reserve University were used for analysis. The EDM technique was used to set the fault, the motor speed was 1797 r/min, the sampling frequency was 12 kHz, and 7800 points were selected for analysis in this paper. The structural parameters of the rolling bearing are shown in Table 1.

4.2 Signal decomposition and screening

Taking the inner ring fault data as an example, the waveforms of the fault signal are shown in Fig. 7a–d. In the time-domain diagram, the signal waveform is relatively noisy, and there is no obvious shock signal. In the spectrogram, there is an obvious modulation phenomenon in the range of 2000–5000 Hz. The time–frequency diagram of the fault signal is densely populated with noise, indicating that it contains more noise. In the envelope spectrum, the characteristic frequency and its multiplier are covered by the rotary frequency and its multiplier as well as the noise interference band, and the weak

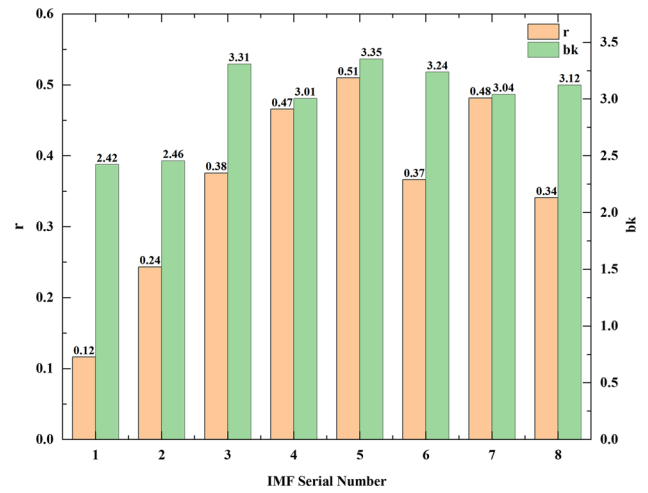


Fig. 8 Correlation coefficients and kurtosis values for IMFs

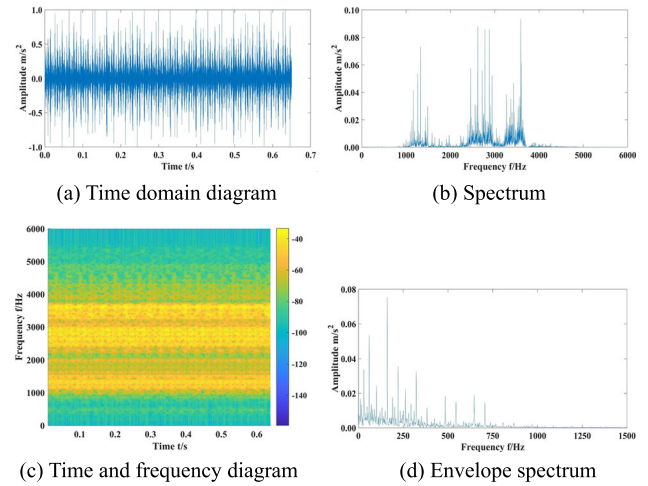


Fig. 9 Bearing reconfiguration signal waveform diagram

pulse characteristics are almost completely ignored, which makes it impossible to carry out fault diagnosis.

Using the method proposed in this paper, the signal is first denoised by SVD, and the optimal number of decomposition layers $K = 8$ is determined based on the singular value kurtosis difference spectrum. The histograms of correlation coefficient r and kurtosis bk for each IMF are shown in Fig. 8. The mean value of the correlation coefficient is 0.36, and the sub-signals IMF3, IMF4, IMF5, IMF6, and IMF7 with r greater than 0.36 and bk greater than 3 are screened for reconstruction.

4.3 Signal reconstruction and enhancement

The waveforms of the reconstructed signals are shown in Fig. 9a–d. In the figure, it can be observed that the shock signal features covered by noise have been revealed after

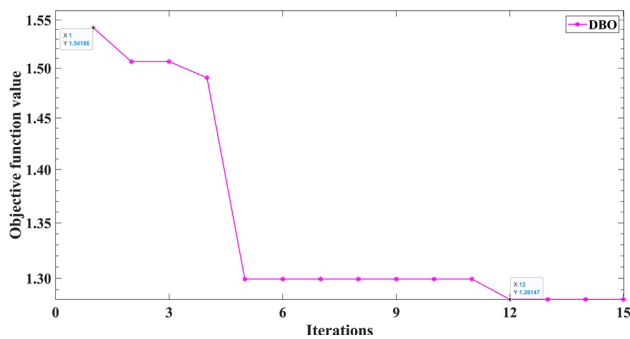


Fig. 10 DBO optimization curve

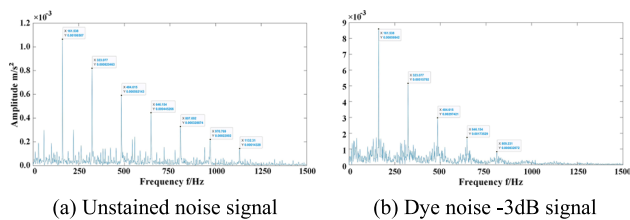


Fig. 11 The envelope spectrum of the inner ring fault signal processed by this method

processing, and the noise in the time–frequency diagram has been reduced significantly, indicating that the proposed method is effective in noise reduction, and it can be seen from the envelope spectrum that the octave of the eigenfrequency is difficult to distinguish.

MCKD is optimized using DBO, the population size of the DBO algorithm is set to 100, and the maximum number of iterations is 15. The fitness curve of DBO is shown in Fig. 10, and the parameters reach the optimum at the 12th iteration, and the optimal parameter combination is [132, 1]. The reconstructed signal is subjected to the MCKD algorithm, and the optimal parameters are set $L = 132$ and $M = 1$ according to the optimal parameters.

4.4 Envelope comparison

The envelope spectrum of the signal processed by the MCKD algorithm with optimized parameters is shown in Fig. 11a, and the time-domain diagram shows that the frequency of the largest value in the diagram is the eigenfrequency of $f_i = 161.538$ Hz, which can be seen in the figure, the eigenfrequency of the fault and its multiplier frequency is obvious and f_i corresponds to the theoretically calculated fault frequency of the inner ring of the bearing, therefore, it can be determined that the fault location of the rolling bearing is in the inner ring of the bearing. To emphasize the effect of noise reduction, random white noise with a signal-to-noise ratio of -3 dB is added to the fault signal of the inner ring of the bearing f_{ir} , and the envelope spectrum processed by

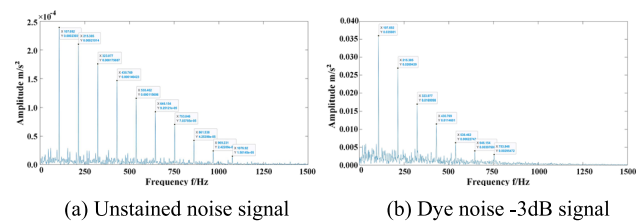


Fig. 12 The envelope spectrum of the outer ring fault signal processed by this method

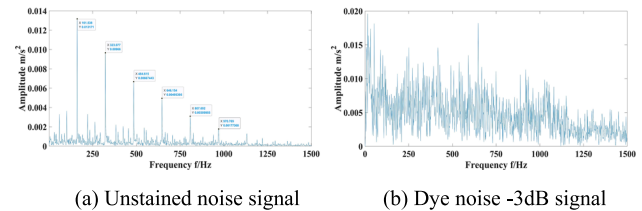


Fig. 13 PE-MCKD processing inner ring fault signal envelope

the method of this paper is shown in Fig. 11b, and it can be seen that the characteristic frequency and its multiplicative frequency are also clearly extracted.

The envelope spectra for the outer bearing signals using the method proposed in this paper are shown in Fig. 12. Where Fig. 12a shows the unstained outer bearing signal and (b) shows the stained signal with -3 dB random white noise added. The MCKD optimized by DBO enhances the weak impulse fault, and the optimization combinations are [235, 1] and [309, 1], respectively, and the frequency opposite to the largest magnitude in the figure is taken as the eigenfrequency $f_i = 107.629$ Hz. The eigenfrequency and its multiplier frequency in the figure are extracted in an orderly manner, with almost no sideband effects, and correspond to the theoretical value of the bearing outer ring fault frequency f_{or} , so it is possible to determine the location of rolling bearing faults in the bearing outer ring.

4.5 Comparison with the PE-MCKD methodology

Liu et al. used an improved MCKD method using the maximum alignment entropy value to determine the optimal filter length L and the optimal fault period T [22]. To verify the superiority of the method in this paper, their proposed PE-MCKD method was used to diagnose the inner ring faults of Case Western Reserve University bearings. Figure 13a shows the untainted noise envelope spectrum processed by the method, and the optimization combination of L and T is [279, 74], in which the fault frequency $f_i = 161.538$ Hz, and its 2–5 octave frequencies can be seen; (b) shows the tainted noise envelope spectrum with the addition of a -3 dB Gaussian white noise, and the optimization combination of L and T is [264, 11], and in which the fault frequency

and its octave frequencies have been masked by the noise and are not recognizable. The fault frequency and its octave have been obscured by noise and cannot be recognized in the graph. This indirectly proves the superiority of the method proposed in this paper.

5 Conclusion

The algorithm proposed in this paper realizes the fault diagnosis of rolling bearing, introduces the SVD to get the singular value matrix of the vibration signal, locates the position of the mutation of the singular value peak difference spectrum to determine the effective order of the singular value matrix, to denoise the vibration signal. In addition, the peak singular value difference spectrum mutation is set as the initial K -value of VMD, and a reasonable K -value is searched according to the optimal K -value algorithm proposed in this paper, which improves the status quo of the K -value setting relying too much on empirical values. The IMF components are screened and signal reconstruction is performed using the principles of kurtosis and correlation. For the first time, the DBO algorithm and the MCKD algorithm are combined to search for the optimal values of the parameters L and M in the MCKD, and the optimized MCKD algorithm is used to enhance the reconstruction of weak pulses in the signal. The experimental results show that the proposed method can effectively remove the noise in the vibration signal, and the K value calculated by the optimal K value algorithm can effectively decompose the signal under the premise of ensuring that no modal aliasing occurs. The DBO optimization algorithm can jump out of the local optimum to find the optimal combination of L and M of the MCKD algorithm, and the experiments verified the reasonableness and validity of the optimization of the MCKD algorithm using the DBO algorithm. Comparison with the PE-MCKD algorithm also confirms that the algorithm proposed in this paper has good noise immunity, effectively extracts the bearing fault characteristics, and determines the fault location in a strong background noise environment.

Author contributions ML is responsible for the entire experiment execution and paper writing. DL is responsible for the review and correction of papers. LY and XW are responsible for guiding the experiment. FZ and YL are responsible for checking and reviewing manuscripts. This study is funded by LY.

Funding This research was funded by the National Natural Science Foundation of China (62203146).

Data availability The datasets generated during and/or analyzed during the current study are available from the corresponding author on reasonable request.

Declarations

Competing interests The authors have no relevant financial or non-financial interests to disclose.

References

- Zhang, J., Zhang, Q., Qin, X., et al.: A two-stage fault diagnosis methodology for rotating machinery combining optimized support vector data description and optimized support vector machine. *Measurement* **200**, 111651 (2022)
- Qian, M., Yu, Y., Guo, L., et al.: A new health indicator for rolling bearings based on impulsiveness and periodicity of signals. *Meas. Sci. Technol.* **33**(10), 105008 (2022)
- Yang, J., Zhou, C.: A fault feature extraction method based on LMD and wavelet packet denoising. *Coatings* **12**(2), 156 (2022)
- Han, D., Zhao, N., Shi, P.: Gear fault feature extraction and diagnosis method under different load excitation based on EMD, PSO-SVM, and fractal box dimension. *J. Mech. Sci. Technol.* **33**, 487–494 (2019)
- Li, H., Liu, T., Wu, X., et al.: Application of EEMD and improved frequency band entropy in bearing fault feature extraction. *ISA Trans.* **88**, 170–185 (2019)
- Wang, L., Shao, Y.: Fault feature extraction of rotating machinery using a reweighted complete ensemble empirical mode decomposition with adaptive noise and demodulation analysis. *Mech. Syst. Signal Process.* **138**, 106545 (2020)
- Zhang, X., Miao, Q., Zhang, H., et al.: A parameter-adaptive VMD method based on grasshopper optimization algorithm to analyze vibration signals from rotating machinery. *Mech. Syst. Signal Process.* **108**, 58–72 (2018)
- Xing, Y.H., Yu, H., Zhang, J., et al.: Research on the O-VMD thickness measurement data processing method based on particle swarm optimization[J/OL]. *Chin. J. Sci. Instrum.* 1–11[2023-06-03].
- Ji, Z.Y., Tang, Q., Li, Y.X., et al.: Power system harmonic analysis under non-stationary situations based on AVMD and improved energy operator. *Chin. J. Sci. Instrum.* **43**(07), 209–217 (2022)
- Tan, C., Yang, L., Chen, H., et al.: Fault diagnosis method for rolling bearing based on VMD and improved SVM optimized by METLBO. *J. Mech. Sci. Technol.* **36**(10), 4979–4991 (2022)
- Miao, Y., Zhao, M., Lin, J., et al.: Application of an improved maximum correlated kurtosis deconvolution method for fault diagnosis of rolling element bearings. *Mech. Syst. Signal Process.* **92**, 173–195 (2017)
- McDonald, G.L., Zhao, Q., Zuo, M.J.: Maximum correlated Kurtosis deconvolution and application on gear tooth chip fault detection. *Mech. Syst. Signal Process.* **33**, 237–255 (2012)
- Hong, L., Dhupia, J.S.: A time domain approach to diagnose gearbox fault based on measured vibration signals. *J. Sound Vib.* **333**(7), 2164–2180 (2014)
- Zhu, X.Y., Wang, Y.J.: Early fault diagnosis of rolling bearings based on autocorrelation analysis and MCKD. *J. Vib. Shock* **38**(24), 183–188 (2019)
- Chen, X., Guo, Y., Wu, X., et al.: Planet bearing outer-race fault diagnosis based on MCKD and improved IESFO gram. *J. Vib. Shock* **40**(20), 200–206 (2021)
- He, Y., Wang, H., Xue, H., et al.: Research on unknown fault diagnosis of rolling bearings based on parameter-adaptive maximum correlation kurtosis deconvolution. *Rev. Sci. Instrum.* **92**(5), 055103 (2021)

17. Faris, H., Aljarah, I., Al-Betar, M.A., et al.: Grey wolf optimizer: a review of recent variants and applications. *Neural Comput. Appl.* **30**, 413–435 (2018)
18. Xue, J., Shen, B.: A novel swarm intelligence optimization approach: sparrow search algorithm. *Syst. Sci. Control Eng.* **8**(1), 22–34 (2020)
19. Xue, J., Shen, B.: Dung beetle optimizer: a new meta-heuristic algorithm for global optimization. *J. Supercomput.* **79**(7), 7305–7336 (2023)
20. Jun, Z.: Diagnosis of multiple faults in rolling bearings based on adaptive maximum correlated kurtosis deconvolution. *J. Vib. Shock* **38**(22), 171–177 (2019)
21. Song, Y.B., Liu, Y.H., Zhu, D.P.: Adaptive UPEMD-MCKD rolling bearing fault feature extraction method. *J. Vib. Shock* **42**(03), 83–91 (2023)
22. Liu, P., Lin, Z., Zhang, M., et al.: Fault diagnosis of rolling bearing based on permutation entropy optimized maximum correlation kurtosis deconvolution. *IOP Conf. Ser. Mater. Sci. Eng.* **1043**(2), 022029 (2021)

Publisher's Note Springer Nature remains neutral with regard to jurisdictional claims in published maps and institutional affiliations.

Springer Nature or its licensor (e.g. a society or other partner) holds exclusive rights to this article under a publishing agreement with the author(s) or other rightsholder(s); author self-archiving of the accepted manuscript version of this article is solely governed by the terms of such publishing agreement and applicable law.